J. Fluid Mech. (2014), *vol.* 741, *pp* 681–701. © Cambridge University Press 2014
doi:10.1017/jfm.2013.13

Non-classical gas dynamics of vapour mixtures

Alberto Guardone[1], Piero Colonna[2,†], Emiliano Casati[2,3] and Enrico Rinaldi[4]

[1]Department of Aerospace Science and Technology, Politecnico di Milano, Via La Masa 34, Milano, 20156, Italy

[2]Propulsion and Power, Delft University of Technology, Kluyverweg 1, Delft, 2629 HS, The Netherlands

[3]Energy Department, Politecnico di Milano, Via Lambruschini 4, Milano, 20156, Italy

[4]Process and Energy Department, Delft University of Technology, Leeghwaterstraat 39, 2628 CB, Delft, The Netherlands

(Received 13 May 2013; revised 5 December 2013; accepted 30 December 2013; first published online 13 February 2014)

The non-classical gas dynamics of binary mixtures of organic fluids in the vapour phase is investigated for the first time. A predictive thermodynamic model is used to compute the relevant mixture properties, including its critical point coordinates and the local value of the fundamental derivative of gas dynamics Γ. The considered model is the improved Peng–Robinson Stryjek–Vera cubic equation of state, complemented by the Wong–Sandler mixing rules. A finite thermodynamic region is found where the nonlinearity parameter Γ is negative and therefore non-classical gas dynamics phenomena are admissible. A non-monotone dependence of Γ on the mixture composition is observed in the case of binary mixtures of siloxane and perfluorocarbon fluids, with the minimum value of Γ in the mixture being always larger than that of its more complex component. The observed dependence indicates that non-ideal mixing has a strong influence on the gas dynamics behaviour, either classical or non-classical, of the mixture. Numerical experiments of the supersonic expansion of a mixture flow around a sharp corner show the transition from the classical configuration, exhibiting an isentropic rarefaction fan centred at the expansion corner, to non-classical ones, including mixed expansion waves and rarefaction shock waves, if the mixture composition is changed.

Key words: compressible flows, gas dynamics, shock waves

1. Introduction

The first scientist who hinted at the possibility of observing rarefaction shock waves (RSWs) in vapours of molecularly complex organic fluids was Nobel-laureate Hans Bethe (1942). RSWs are discontinuous solutions to the Euler equations of compressible flows where the fluid undergoes an irreversible expansion process which results into a discontinuous reduction of density, pressure, temperature and fluid velocity in the direction of propagation of the shock wave. As is well known, RSWs are not physically admissible in dilute gases with constant specific heats.

† Email address for correspondence: P.Colonna@TUDelft.nl

https://doi.org/10.1017/jfm.2013.13 Published online by Cambridge University Press

In a broad theoretical study on the theory of shock waves in arbitrary material, Bethe outlined how the occurrence of RSWs depends on a peculiar combination of the thermodynamic properties of the material at the states of interest. He noticed that according to the van der Waals (1988) model, RSWs would theoretically be possible in the dense vapour of fluids featuring high values of the heat capacity, if the pre- and post-shock states of the fluid are close to the vapour–liquid critical point. Nevertheless, he ruled out this possibility on the grounds of what we now know as incorrect physical arguments, see also Thompson & Lambrakis (1973). An early contribution is also due to Zel'dovich (1946) and Weyl (1949). However, it was Thompson (1971) (see also Thompson & Lambrakis 1973; Thompson 1988), who first provided a systematic treatment of what is now called non-classical gas dynamics. A review article by Kutateladze, Nakoryakov & Borisov (1987) documents the advancements in non-classical gas dynamics until the 1980s, while a more recent review can be found in Kluwick (2001).

A necessary condition for non-classical behaviour to be physically admissible is that the fundamental derivative of gas dynamics

$$\Gamma \equiv 1 + \frac{\rho}{c}\left(\frac{\partial c}{\partial \rho}\right)_s = \frac{v^3}{2c^2}\left(\frac{\partial^2 P}{\partial v^2}\right)_s, \tag{1.1}$$

a thermodynamic property of the fluid first introduced by Hayes (1960), is negative. In definition (1.1), ρ is the density, s is the entropy, P is the pressure, $v = 1/\rho$ is the specific volume and c is the zero-frequency speed of sound $c \equiv (\partial P/\partial \rho)_s$. If Γ is negative in a finite thermodynamic region, RSWs are admissible, among other so-called non classical waves such as composite and split waves, see, e.g., Thompson (1971).

Substances characterized by thermodynamic states featuring negative values of Γ in the dense vapour phase are called Bethe–Zel'dovich–Thompson (BZT) fluids. The region of negative Γ in the vapour phase is shown in figure 1 in the pressure–specific volume thermodynamic diagram of a paradigmatic BZT fluid described by the van der Waals fluid model, where the $\Gamma = 0$ line and the vapour saturation line delimit the negative-Γ region. The studies of Thompson sparked quite some interest in the following years, and many investigations expanded the theory covering several non-classical phenomena and aspects, see e.g. Cramer & Kluwick (1984), Cramer & Sen (1986, 1987), Menikoff & Plohr (1989), Cramer (1989), Cramer & Sen (1990), Cramer & Crickenberger (1991), Cramer (1991) and Kluwick & Meyer (2010). One of the latest developments is related to the investigation of non-classical phenomena in the vapour–liquid critical point region of any common fluid (see Nannan, Guardone & Colonna 2013).

Experimental evidence of non-classical gas dynamics is available only for two-phase vapor–liquid (see Thompson, Carofano & Kim (1986), Gulen, Thompson & Cho (1989), and Thompson (1991)) or solid–solid systems, see Ivanov & Novikov (1961). In the single-phase vapour region, only classical gas dynamics phenomena have been observed so far. Notably, in the former Soviet Union, Borisov *et al.* (1983) made an attempt to experimentally prove the existence of a RSW, using a special shock tube. The interpretation of the results of the experiments, arguably a RSW front developing in the tube, has later been confuted in the light of additional knowledge and simulation capability (Fergason 2001; Kluwick 2001; Nannan *et al.* 2013). Theoretical studies (Chandrasekar & Prasad 1991; Cramer, Tarkenton & Tarkenton 1992; Schnerr & Molokov 1994, 1995; Aldo & Argrow 1995; Brown & Argrow

https://doi.org/10.1017/jfm.2013.13 Published online by Cambridge University Press

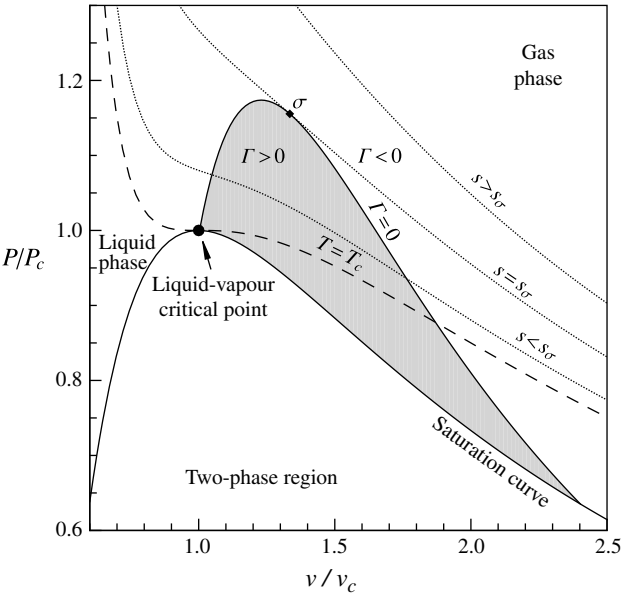


FIGURE 1. From Guardone, Zamfirescu & Colonna (2010). Liquid–vapour saturation curve (—) and $\Gamma < 0$ region (shaded region) for a BZT fluid in the volume-pressure plane computed from van der Waals model under the assumption of a constant isochoric specific heat c_v and for $c_v/R = 2000$, with R gas constant. Selected isentropes ($\cdots$) and the critical isotherm $T = T_c$ ($-\ -$) are also indicated. Note that the isentropes are concave down in the $\Gamma < 0$ region. The isentrope s_σ is tangent to the $\Gamma = 0$ line in σ.

1998), and new simulation capabilities (Schnerr & Leidner 1993*a*,*b*; Argrow 1996; Monaco, Cramer & Watson 1997; Brown & Argrow 1997, 2000; Cinnella & Congedo 2007, 2008; Cinnella 2008), paved the way to a new experimental attempt in 2000 at the University of Boulder (Fergason 2001; Fergason *et al.* 2001; Fergason, Guardone & Argrow 2003). The failed experiment put into evidence one of the major obstacles, namely that the BZT thermodynamic region (the region comprising the states featuring negative-Γ, see figure 1) is very close to the thermal decomposition temperature of suitable organic fluids, which is in the range 350–400 °C. In addition, the repeatable rupture of the shock-tube diaphragm proved unattainable due to the relatively small pressure difference and the large acoustic impedance of the fluid (Thompson & Loutrel 1973; Guardone 2007; Colonna *et al.* 2008*a*).

Much attention has recently been devoted to the identification of BZT fluids, and to the computation of the negative-Γ region, see Colonna *et al.* (2009) for a review. More recently Colonna *et al.* (2008*a*) started a new project aimed at the generation and measurement of a RSW in a newly conceived Ludwieg-tube-type set-up. A siloxane fluid, D_6 (dodecamethylcyclohexasiloxane $C_{12}H_{36}O_6Si_6$), has initially been selected as the working fluid. Siloxanes are especially suited to the RSW experiment because of available knowledge on their thermal stability (Angelino & Invernizzi 1993; Colonna 1996), thermodynamic properties (Colonna *et al.* 2006; Nannan *et al.* 2007; Colonna, Nannan & Guardone 2008*b*; Nannan & Colonna 2009), and their use as working fluids in thermal energy conversion systems, see e.g. Angelino & Colonna (1998), Uusitalo *et al.* (2013) and Lang, Almbauer & Colonna (2013). Few of the

https://doi.org/10.1017/jfm.2013.13 Published online by Cambridge University Press

compounds of the siloxane family are candidate BZT fluids (Colonna, Guardone & Nannan 2007).

The design of the RSW experiment drove studies aimed at better identifying the thermodynamic region within which non-classical phenomena are admissible (Zamfirescu, Guardone & Colonna 2008), and the maximum pressure difference and shock wave Mach number that can be expected (Guardone *et al.* 2010). Given that the experimental conditions are difficult to realize and that the RSW is expected to be weak, therefore more challenging to measure, uncertainty quantification applied to flow simulations has been preliminarily used as an aid in determining the optimal experimental conditions (Congedo *et al.* 2012).

The present work is motivated by several observations about mixtures of organic fluids. Differently from mixtures of ideal gases, thermodynamic properties of dense vapours of multicomponent mixtures do not scale linearly with the mole fractions of each compound, as molecular interaction among different molecules plays a major role. Typical hallmarks of non-ideal behaviour of fluids mixtures are the critical temperature, pressure and specific volume of a binary mixture, which usually differ from that of each of the constituents. The same holds for the melting point and for most thermodynamic properties. The fundamental derivative of gas dynamics Γ, being a derived thermodynamic property, is also affected by non-ideal mixing effects, as preliminarily discussed in Colonna & Silva (2003). In addition, experiments on the thermal stability of siloxane mixtures (Angelino & Invernizzi 1993; Colonna 1996), and a deeper understanding on the chemistry of thermal decomposition of poly-dimethyl siloxanes (Dvornic 2004), show that, at temperatures close to the so-called temperature stability limit, a pure siloxane undergoes a transformation called *rearrangement*, whereby small quantities of other compounds of the same family are formed. Such mixture composition remains then constant at that temperature over time. The composition of the mixture is therefore a new relevant variable in the study of BZT fluids and, importantly, mixtures of organic fluids are also considered for applications in organic Rankine cycle (ORC) power systems (Angelino & Colonna 1998, 2000; Chen *et al.* 2011; Trapp & Colonna 2013), one of the possible applications of non-classical gas dynamics (Brown & Argrow 2000).

In the present preliminary study on mixtures as BZT fluids, siloxanes and perfluorocarbons have been considered as constituents. Suitable thermodynamic models for multicomponent fluids are briefly discussed in § 2. Their limitation in terms of accuracy of the predicted Γ values is also addressed. These models are used to estimate the boundaries of the thermodynamic region of admissibility of RSWs, and the influence of the mixture composition. In § 3, exemplary simulation of a supersonic flow expanding over a wedge, whereby the composition of the mixture is varied, are presented to assess the influence of the molecular composition on the gas dynamics behaviour. Concluding remarks and an outlook on future research are given in § 4.

2. Admissibility region for RSWs in dense gas mixtures

Modelling non-ideal thermodynamic properties of fluid mixtures, including the determination of the fundamental derivative of gas dynamics Γ, requires to correctly account for the interaction between different molecules, an added degree of difficulty with respect to pure-fluid thermodynamics. No fundamental and general theory on the interaction of molecules of different type exists yet, therefore no accurate model is available. For these reasons the estimation of mixture properties is affected in

https://doi.org/10.1017/jfm.2013.13 Published online by Cambridge University Press

general by larger uncertainties, if compared to the estimation of pure-fluid properties. Mixtures of simple molecules, e.g. light gases and simple hydrocarbons, can be modelled with relatively high accuracy, and reference equations of state (EoSs) have been developed (Kunz *et al.* 2007). These semi-empirical models rely on large sets of accurate fluid property measurements. Unfortunately, accurate property measurements of complex organic compounds are not available. In order to estimate dense-vapour thermodynamic properties of mixtures of complex organic fluids, simpler so-called predictive EoSs must be adopted (see e.g. Sandler 1989, 1993). These models rely on a small set of data related to the pure constituents, and to parameters describing the interaction between different molecules; these parameters can be determined either experimentally or estimated. Predictive models applicable to mixtures are thermodynamically consistent, but calculated property values are affected by much larger uncertainties if compared with the estimation of pure-fluid properties.

In this study the properties of mixtures of siloxanes and perfluorocarbons are evaluated with either the improved Peng–Robinson Stryjek–Vera cubic EoS (van der Stelt, Nannan & Colonna 2012), complemented by the Wong–Sandler mixing rules (iPRSV-WS; see Wong & Sandler 1992; Coutsikos, Kalospiros & Tassios 1995), or the perturbed-chain statistical associating fluid theory (PC-SAFT) model (Gross & Sadowski 2001), which is formulated in terms of molecular parameters whose value depends on the molecular arrangement. Since most of the treatment in this paper is based on the use of the iPRSV-WS model, both the functional form of the EoS and the derivation of the adopted mixing rules are recalled in Appendix A. These models, together with others, are implemented in an in-house computer library for the calculation of primary and secondary thermodynamic properties of fluids (Colonna 2012).

Information on how the data for the iPRSV-WS model applied to siloxane mixtures were obtained can be found in Angelino & Colonna (1998). The analytical expression of Γ for this thermodynamic model is reported in Colonna & Silva (2003). The application of the PC-SAFT model to linear siloxanes is documented in Lai, Wendland & Fischer (2009), and has been extended by the authors to model also cyclic siloxanes. Siloxane/perfluorocabon mixtures are modelled with the iPRSV-WS EoS starting from experimental values of the critical point of these mixtures (Armenio 2009), and compared with results from the PC-SAFT model. Such a comparison is the only possible assessment at the moment, since no other experimental values are available. Values of Γ for the PC-SAFT mixture model are calculated with analytical expressions obtained by derivation from the EoS and the isobaric ideal-gas heat capacity relation, see for example Colonna *et al.* (2009) and Nannan *et al.* (2013).

Figure 2 shows a comparison between the values of Γ calculated along the dew line for the equimolar mixture of propane and pentane using a reference model (Kunz *et al.* 2007), the iPRSV-WS and the PC-SAFT models. As it is known, Abbott (1973), Bymaster *et al.* (2008), predictive models fail to accurately estimate properties close to the vapour–liquid critical point, therefore also Γ values at high reduced temperature $\tilde{T} = T/T_c$ deviate from those obtained with the reference model, cf. figure 2. A number of evaluations for various fluids modelled by the reference model of Kunz *et al.* (2007) revealed that the iPRSV-WS model performs better than the PC-SAFT model in the critical-point region, therefore it has been chosen for the analysis presented in § 3.

Figure 3 shows the negative-Γ region (also termed the BZT region) in the P–T thermodynamic plane for several selected organic compounds of the family of siloxanes, fluorocarbons, perfluorocarbons and their mixtures, calculated with the iPRSV-WS model. The ensemble of fluid thermodynamic states featuring a negative

https://doi.org/10.1017/jfm.2013.13 Published online by Cambridge University Press

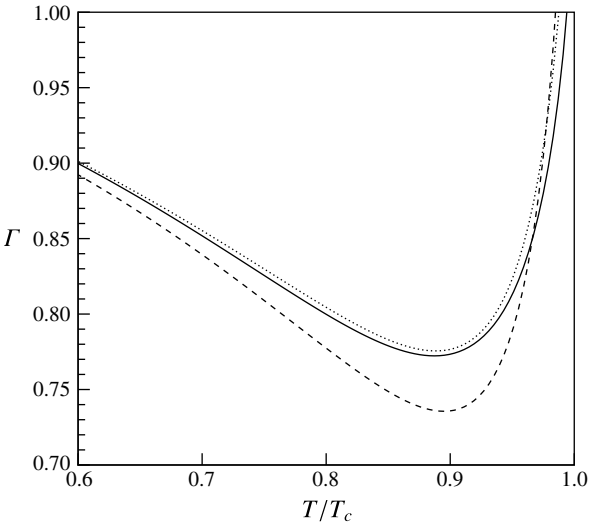


FIGURE 2. Comparison of Γ values along the dew line as a function of the reduced temperature T/T_c for the equimolar mixture of propane and pentane calculated with the reference model by Kunz *et al.* (2007) (—), the iPRSV-WS (· · ·), and PC-SAFT (– – –) thermodynamic models.

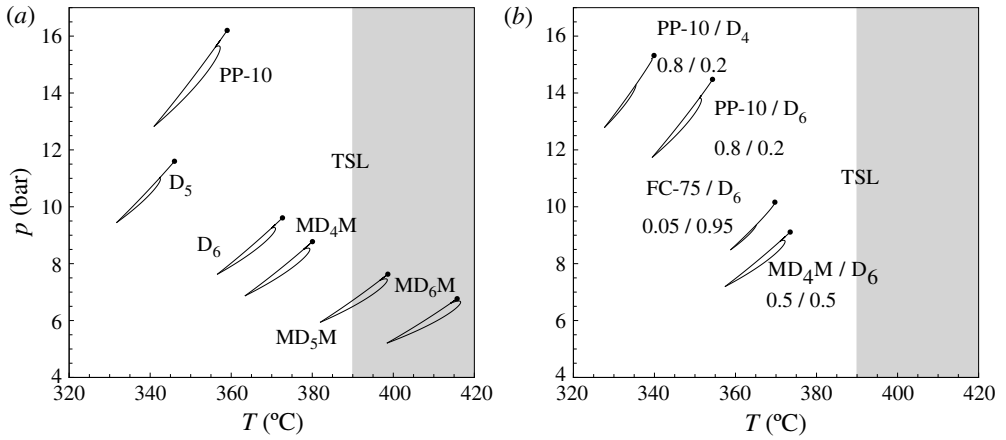


FIGURE 3. Negative Γ region (or BZT region) in the P–T thermodynamic plane for several pure fluids (*a*) and some selected mixtures (*b*) values are calculated with the iPRSV-WS thermodynamic model. For each fluid, the circle indicate the critical point. It is relevant to future experiments on non-classical gas dynamic phenomena that the temperature values are close to the estimated thermal stability limit (TSL) for these organic compounds in contact with stainless steel (≈390 °C), while the values of pressure are comparatively moderate. The shaded area indicates the range of temperatures where thermal decomposition in stainless steel can be expected.

value of Γ in the dense vapour phase is delimited by the dew line on the left and by the concave-upward $\Gamma = 0$ line on the right. An estimate of the temperature at which thermal breakdown in stainless steel is likely to occur is also indicated (thermal stability limit, TSL).

https://doi.org/10.1017/jfm.2013.13 Published online by Cambridge University Press

x		MW	P_c	T_c	ρ_c	Γ_{min}
MDM	MD_6M	(g mole^{-1})	(bar)	(K)	(kg m^{-3})	(–)
1.00	0.00	236.5	14.2	564.1	229.38	0.0917
0.75	0.25	329.2	18.0	653.9	288.41	0.5676
0.40	0.60	459.0	11.7	687.5	260.34	0.2567
0.15	0.85	551.7	8.3	690.3	243.09	−0.1187
0.05	0.95	588.8	7.2	689.6	236.65	−0.3040
0.00	1.00	607.3	6.8	689.0	230.64	−0.4001

TABLE 1. Molar fraction x, average molecular weight MW, critical pressure P_c, critical temperature T_c, critical density ρ_c and minimum value of the fundamental derivative of gas dynamics Γ_{min} for a mixture of siloxane fluids MDM and MD_6M.

As an example, in table 1, the molar fraction x, average molecular weight MW, critical pressure P_c, critical temperature T_c, critical density ρ_c and minimum value of the fundamental derivative of gas dynamics Γ_{min} for the mixture of siloxane fluids MDM and MD_6M are reported. Thermodynamic properties are calculated using the iPRSV-WS thermodynamic model. As is well known, the critical point coordinates in table 1 depend in a nonlinear fashion on the mixture composition x, with the critical pressure, temperature and density exhibiting a local maximum.

Admittedly, the negative-Γ region of fluids MD_5M and MD_6M is partially or completely past the TSL, see figure 3. Although mixtures are expected to be more thermally stable than their pure components, such high values of operating temperatures are unrealistic, if stainless steel is the containing material. Moreover, for MD_5M and MD_6M the negative-Γ region is very close to the liquid–vapour saturation point, where the value of Γ is expected to diverge to infinity (Nannan *et al.* 2013). In this region, an accurate evaluation of the thermodynamic properties, including Γ, would require the inclusion of a critical point scaling law and of a cross-over model, linking the latter with the analytical EoS. In the present qualitative study fluid, MD_6M was considered in order to maximize the strength of non-classical phenomena for illustration purposes; thermal decomposition and critical point effects are to be carefully assessed before selecting this fluid for the experiments. However, it is remarkable that, similarly to previous studies on non-classical gas dynamics, the present findings are directly applicable to less-complex molecules, because the qualitative fluid dynamic behaviour is similar to that of MD_6M.

Results shown in figure 4 are a preliminary evaluation of the dependence of the minimum value of Γ on the molecular weight and on the molecular complexity, which is defined here as the equivalent number of active translational, rotational and vibrational degrees of freedom of the molecules at the critical temperature and in the dilute gas limit (see Colonna & Guardone 2006). The molar composition is also indicated for mixtures. As it is known, in the case of pure fluids the minimum value of Γ along the dew line, Γ_{min}, decreases monotonically with increasing molecular weight and complexity (figure 4*a*). In addition, the extension of the BZT region in the P–T plane increases with increasing molecular weight and complexity, cf. figure 3(*a*).

It is remarkable that the effect of mixing, therefore of intermolecular interaction, alters the non-monotone dependency of Γ_{min} from molecular weight and complexity. Figure 4(*b*) shows that for binary mixtures of the siloxane fluids MDM/MD_6M and MD_5M/MD_6M the estimated value of Γ_{min} does not decrease monotonically with

https://doi.org/10.1017/jfm.2013.13 Published online by Cambridge University Press

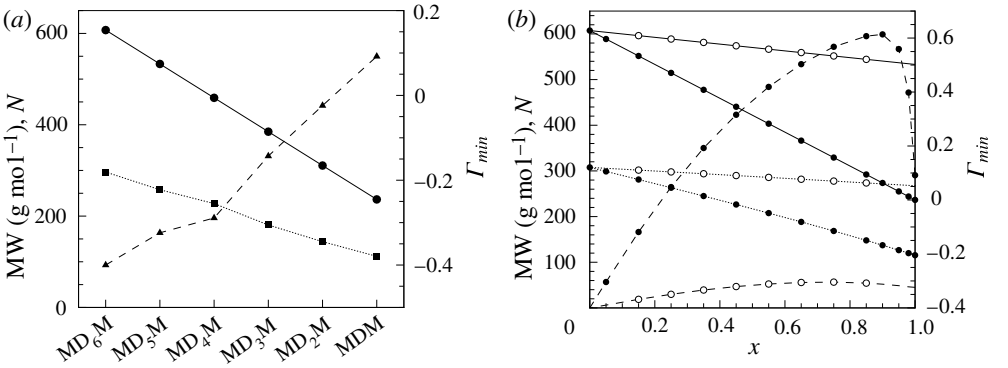


FIGURE 4. Molecular weight MW (—), active degrees of freedom evaluated at the critical temperature N (· · ·) and minimum value of Γ along the dew line (– – –) for selected linear siloxanes. Properties are calculated with the iPRSV EoS for the pure fluids (see van der Stelt 2012), while the EoS is complemented by the Wong–Sandler mixing rules (Wong & Sandler 1992) for the mixtures. (a) Pure linear siloxanes. (b) Values for mixtures of MDM/MD_6M (•) and MD_5M/MD_6M (○).

increasing average molecular complexity and weight of the mixture, similarly to what observed for the values of the critical pressure, temperature and density in table 1. Indeed, for both the MDM/MD_6M and the MD_5M/MD_6M mixtures, the value of $\Gamma_{\min}$ exhibits a maximum, which is at $x_{\mathrm{MDM}} \approx 0.75$ for MDM/MD_6M, and at $x_{\mathrm{MD_5M}} \approx 0.9$ for MD_5M/MD_6M. Notably, for the mixture MDM(0.4)/MD_6M(0.6) the value of $\Gamma_{\min}$ is largely different, even in sign, from that predicted for MD_4M, which is the homologous pure fluid in terms of molecular weight and complexity. This type of dependency of $\Gamma_{\min}$ on molar composition is predicted also in case of mixtures of alkanes, by using reference EoSs for the calculation of thermodynamic properties.

In the case presented here, the variation of $\Gamma_{\min}$ with the mole fraction of a binary mixture is such that, for any given composition, $\Gamma_{\min}$ is always larger than the molar-fraction-averaged value of $\Gamma_{\min}$ of the two pure constituents. Owing to the large variety of intermolecular forces, it cannot currently be ruled out that an opposite trend can be observed for different combinations of pure fluids, namely that the mixing of two or more fluids not considered here leads to values of $\Gamma_{\min}$ that are lower than those of the mixture constituents.

From the knowledge of the fundamental derivative of gas dynamics in the vapour phase, the thermodynamic conditions resulting in non-classical gas dynamics waves can be determined. The conditions for the admissibility of rarefaction shocks are given by Zamfirescu *et al.* (2008), where the method for determining the so-called *rarefaction shock region* (RSR) is also reported.

In figure 5(*a*) the RSR of siloxane fluid MD_6M is shown, together with a representative isentrope $s = s_{\mathrm{A}}$. As detailed in Zamfirescu *et al.* (2008), the RSR is the thermodynamic region that includes all of the states that can possibly be upstream and downstream of a RSW. By definition, the RSR embeds the negative-Γ region. For pure fluids, the size of the RSR increases with molecular complexity, similarly to the BZT region. In particular, the RSR is limited by the vapour–liquid saturation (VLE) curve and by the double sonic line (DSL), which is the locus of all fluid states that can be connected by a double sonic shock, whereby the pre- and post-shock states are sonic. The DSL and the VLE are connected by the two loci

https://doi.org/10.1017/jfm.2013.13 Published online by Cambridge University Press

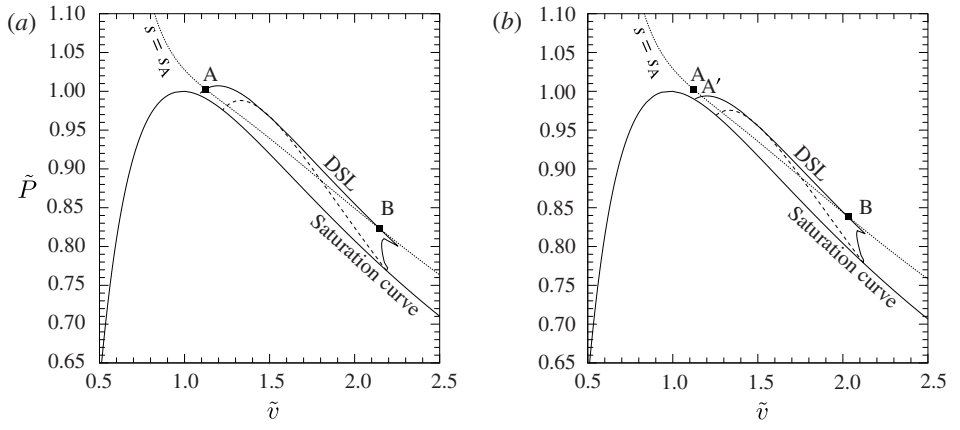


FIGURE 5. (*a*) Pre- and (*b*) post-expansion states on the reduced P–v plane. The negative-Γ region (dashed line) and DSL are also reported: (*a*) MD6M; (*b*) MDM(0.05)/MD_6M (0.95).

representing the upstream state of upstream-sonic downstream-saturated rarefaction shocks and the downstream state of upstream-saturated downstream-sonic RSW.

Each isentrope intersects the DSL in two points A and B, with $v_A < v_B$. At point A the Rayleigh line connecting point A and B is tangent to both the isentrope trough A and the shock adiabat trough A. At point B, it is tangent to the isentrope trough B and the shock adiabat trough A. Therefore, the shock connecting point A and B is a double sonic shock, with sonic state in both point A and B. The RSW connecting point A and B encompasses the largest possible pressure difference, i.e. is the strongest possible RSW originating from the considered isentrope. Note that in figure 5(*a*) the shock adiabat through A and the isentrope $s = s_A$ are not distinguishable.

The RSR of mixtures is calculated with the same procedure as for pure fluids, with no modifications. An example is given in figure 5(*b*), where the RSR for the mixture MDM(0.05)/MD_6M(0.95) is shown. The increase of the MDM percentage in the mixture MDM/MD_6M causes the RSR to reduce its size in the P–v plane, if compared with that of pure MD_6M.

3. Non-classical gas dynamics behaviour of dense gas mixtures

A preliminary study on the effect of the mixture composition on the gas dynamic behaviour of mixtures of organic fluids has been carried out. To this purpose, the supersonic expansion of the dense vapour of a mixture over a corner is simulated.

The selected mixture is composed of MD_6M, a BZT fluid, and MDM, a fluid for which no suitable thermodynamic model predicts a negative-Γ region. To compare results for different mixture composition, a common upstream state was selected in terms of dimensionless quantities. The upstream state features the same value of the Mach number M, reduced pressure $\tilde{P} \equiv P/P_c$ and non-dimensional entropy $\tilde{s} = s/s_\tau$ for all simulations. The locus $s = s_\tau$ is the isentrope tangent to the saturation line, see figure 5. The choice of $\tilde{P}$ and $\tilde{s}$ to identify the upstream flow state is motivated by the fact that they identify homologous thermodynamic states in the P–v thermodynamic plane, with comparable real gas effects.

https://doi.org/10.1017/jfm.2013.13 Published online by Cambridge University Press

M_A	$\tilde{s}_\mathrm{A}$	$\tilde{P}_\mathrm{A}$
1.15470	1.00276	1.00217

TABLE 2. Upstream states for the simulations of the supersonic flow of a dense gas mixture over an expansion corner.

The values of M, $\tilde{P}$ and $\tilde{s}$ identifying the upstream states for the simulations are reported in table 2. The solid surface past the corner forms an angle of $-13.169°$ with respect to the free-stream direction. These values have been chosen so that in the case of pure MD_6M a RSW with maximum intensity is obtained, which forms an angle of 60° with respect to the free-stream direction (see Guardone *et al.* 2010).

The computer program used to perform the simulations is a parallel solver for the Navier–Stokes equations on unstructured meshes based on a finite volume formulation and implicit time-integration (Pecnik *et al.* 2012). The code has been recently extended to include real gas properties (Pecnik, Rinaldi & Colonna 2012) using a general interface to several thermodynamic libraries (Colonna 2012). An unstructured mesh refinement technique is adopted to increase the accuracy in regions where the solutions exhibit the largest gradients.

Figure 6 shows the flow field isobars from flow simulations for different mixtures of MDM/MD_6M, whereby the mole fraction of MDM varies from $x_\mathrm{MDM} = 1$ in figure 6(*a*) to $x_\mathrm{MDM} = 0$ in figure 6(*f*), under the assumption of negligible fluid viscosity and thermal conductivity.

Figure 6(*a*) displays the supersonic flow of a pure MDM vapour. As expected, since $\Gamma > 0$, a classical isentropic expansion fan is observed in this case. It is remarkable that, differently from supersonic expansions of a constant specific heats ideal gas, the Mach number M variation across the expansion is non-monotone, as it can be appreciated from figure 7, where the Mach number is depicted for a representative streamline across the expansion wave. The present non-monotone behaviour is consistent with the value of the parameter J, namely

$$J(s, \rho, M) = 1 - \Gamma(s, \rho) - \frac{1}{M^2}, \tag{3.1}$$

across the expansion wave. Indeed, for isentropic processes from a given state A one has (see Cramer & Best 1991),

$$\frac{\mathrm{d}M}{\mathrm{d}\rho} = J(s_\mathrm{A}, \rho, M)\frac{M}{\rho}. \tag{3.2}$$

As shown in figure 7(*b*), in the expansion of pure MDM vapour depicted in figure 6(*a*), J can have both negative and positive values and therefore M is non-monotone. Note that for a constant specific heat ideal gas, $J = (1-\gamma)/2 - 1/M^2 < 0$, with γ ratio of the isobaric and isochoric specific heats, and therefore M always increases monotonically during a supersonic expansion.

A reversed, non-classical, behaviour is observed for the supersonic expansion of pure MD_6M, shown in figure 6(*f*). An oblique non-classical RSW, which forms an angle of 60° with respect to the upstream flow direction, is observed.

Intermediate situations are observed in the case of mixtures of MDM/MD_6M, shown in figure 6(*b–e*), where the supersonic expansions of mixtures of increasing concentration of the more complex component MD_6M are depicted.

https://doi.org/10.1017/jfm.2013.13 Published online by Cambridge University Press

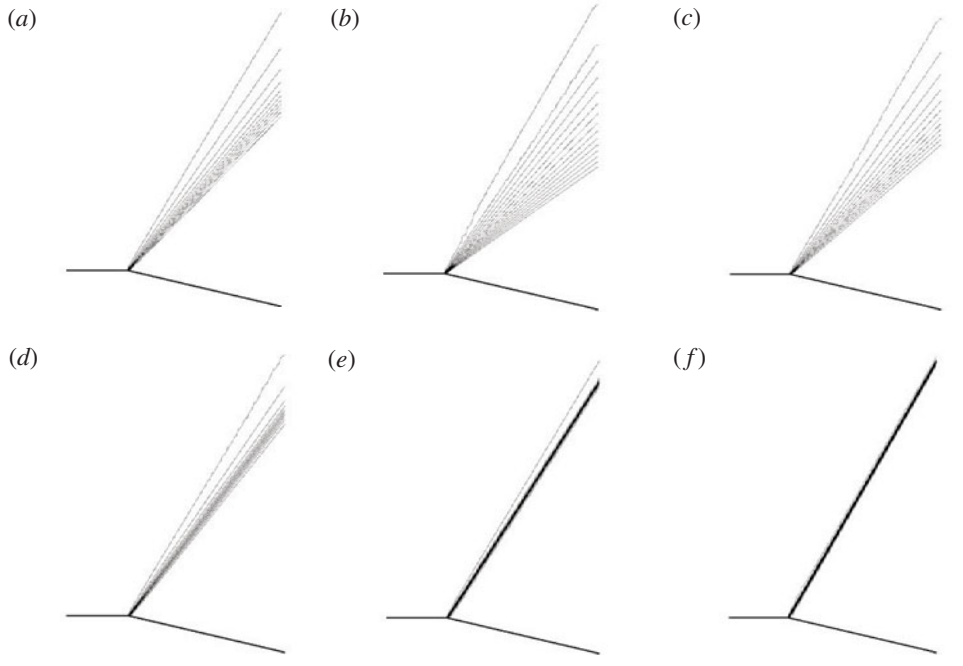


FIGURE 6. Simulated flows of dense vapours of MDM/MD_6M expanding over a corner, whereby the mole fraction of MDM varies from 1 (*a*) to 0 (*f*). There are 15 levels of isopressure contour lines plotted in the range $\tilde{P} = [0.8, 1]$. The upstream state features the same Mach number M, reduced pressure $\tilde{P} \equiv P/P_c$ and reduced entropy $\tilde{s} = s/s_\tau$ in all cases, see table 2. The fluid thermodynamic model is the iPRSV EoS complemented by the Wong–Sandler mixing rules for the mixtures: (*a*) MDM; (*b*) MDM (0.75)/MD_6M (0.25); (*c*) MDM (0.40)/MD_6M (0.60); (*d*) MDM (0.15)/MD_6M (0.85); (*e*) MDM (0.05)/MD_6M (0.95); (*f*) MD_6M.

In particular, in figure 6(*b*), where the flow of a MDM(0.75)/MD_6M(0.25) mixture is shown, a classical rarefaction fan is observed since $\Gamma > 0$. The angular sector encompassed by the fan is larger than that observed in figure 6(*a*) for pure fluid MDM, although the final turning angle $\theta_B = -13.169°$ is the same in both conditions. Therefore, since the slope of the limiting characteristic line at the right boundary of the fan is $\lambda(\theta_B) = \tan(\theta_B + \mu(\theta_B))$ where $\sin \mu_B = 1/M_B$, one can conclude that the Mach number at the end of the expansion is larger in this case, as it is confirmed also by the values in tables 3 and 4. The above can be explained by recalling the dependence of the Mach number on the local velocity angle θ given by the Prandtl–Meyer relation (see Thompson 1988), namely,

$$\mathrm{d}\theta = \frac{\sqrt{M^2 - 1}}{1 - (\Gamma - 1)\, M^2}\, \mathrm{d}M. \tag{3.3}$$

Indeed, despite the larger average molecular weight, along the considered isentrope the value of J for the mixture is always lower than that computed for pure MDM, see figure 7(*b*), and the Mach number difference between the upstream and downstream state is larger.

https://doi.org/10.1017/jfm.2013.13 Published online by Cambridge University Press

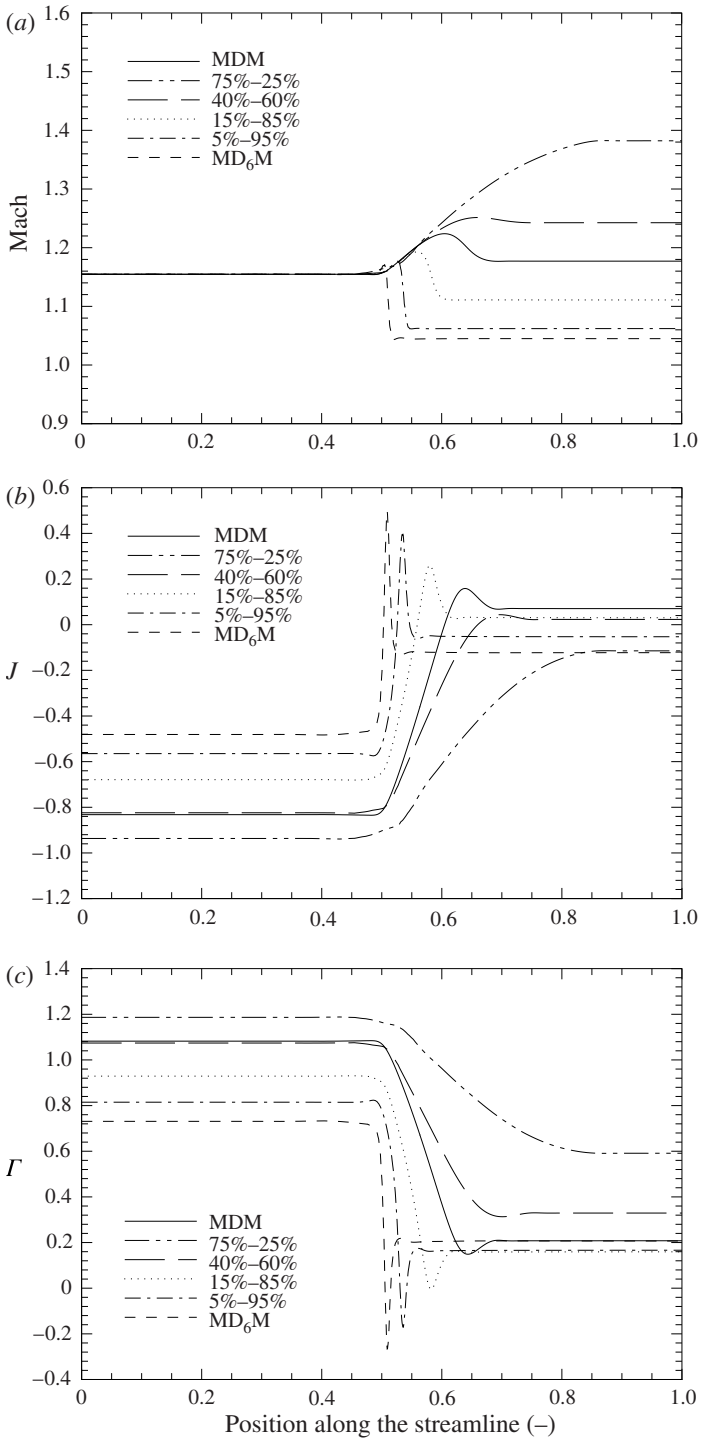


FIGURE 7. Variation of the Mach number (top), the parameter $J = 1 - \Gamma - 1/M^2$ (middle) and Γ (bottom) along a streamline. Different lines correspond to different compositions of the mixture MDM/MD_6M: (*a*) Mach number; (*b*) $J = 1 - \Gamma - 1/M^2$; (*c*) Γ.

https://doi.org/10.1017/jfm.2013.13 Published online by Cambridge University Press

Composition x		Upstream state A				Downstream state B				
MDM	MD_6M	$\tilde{T}_A$	$\tilde{\rho}_A$	Γ_A	Z_A	$\tilde{P}_B$	$\tilde{T}_B$	$\tilde{\rho}_B$	Γ_B	Z_B
1.00	0.00	1.0008	0.8630	1.0823	0.3610	0.8461	0.9833	0.5279	0.2078	0.5072
0.75	0.25	1.0133	0.8280	1.1866	0.4510	0.7764	1.0013	0.5172	0.5912	0.5661
0.40	0.60	1.0027	0.9234	1.0741	0.3912	0.8284	0.9931	0.5698	0.3292	0.5291
0.15	0.85	1.0012	0.9059	0.9290	0.3617	0.8485	0.9919	0.5342	0.1593	0.5241
0.05	0.95	1.0008	0.8785	0.8148	0.3577	0.8382	0.9910	0.4920	0.1664	0.5395
0.00	1.00	1.0005	0.8824	0.7310	0.3532	0.8231	0.9902	0.4660	0.2068	0.5551

TABLE 3. Upstream and downstream thermodynamic states for the different mixtures considered in the simulations. Z is the compressibility factor defined as $Z = RT/Pv$.

Composition x						
MDM	MD_6M	M_B	$\Delta P/P_A$	$\Delta T/T_A$	$\Delta\rho/\rho_A$	$\Delta u/u_A$
1.00	0.00	1.1770	−0.1562	−0.0175	−0.3927	0.4128
0.75	0.25	1.3822	−0.2257	−0.0119	−0.3760	0.3222
0.40	0.60	1.2426	−0.1739	−0.0096	−0.3843	0.3752
0.15	0.85	1.1109	−0.1539	−0.0093	−0.4140	0.4943
0.05	0.95	1.0621	−0.1641	−0.0098	−0.4483	0.6195
0.00	1.00	1.0450	−0.1792	−0.0103	−0.4765	0.7283

TABLE 4. Downstream Mach number and pressure, temperature, density and velocity differences across the expansion waves, where $\Delta(\cdot) = (\cdot)_B - (\cdot)_A$.

In the conditions depicted in figure 6(*c*,*d*), $\Gamma_{min} > 0$, see figure 3 and table 1, and therefore a classical flow is observed in both cases. In figure 6(*c*), the Mach number in state B is larger than that observed in figure 6(*a*), consistently with the Γ and J profiles across the expansion, see figure 7(*c*,*b*), respectively. As a consequence, the angle encompassed by the rarefaction fan is larger than that observed for pure fluid MDM. The opposite situation is found in the case in figure 6(*d*) and the fan is narrower than its pure fluid counterpart.

From table 1 and figure 4, for small concentrations of MDM ($x_{MDM} < 0.15$), Γ assumes negative values in the vapour phase and non-classical behaviour is admissible. This is the case of the flow of mixture MDM(0.05)/MD_6M(0.95) in figure 6(*e*), where the expansion occurs through a non-classical composite wave made of a continuous fan that is terminated by a non-classical RSW, with close-to-sonic downstream state. The expansion is depicted in the thermodynamic plane in figure 5(*b*), which displays the pre- and post-expansion states A and B in the reduced P–v plane. While for the case of the pure fluid MD_6M a single RSW connects the two states, in the case of the mixture MDM(0.05)/MD_6M(0.95), an initial isentropic expansion is observed from state A to state A′, which lies on the DSL. Then, a RSW expands the fluid from A′ to B.

Results are summarized in table 4, which displays the downstream Mach number M and the variations of pressure P, the temperature T, the density ρ and the velocity u across the waves for all of the considered different mixture compositions. The entropy difference across composite waves and the RSW is very small, due to both the relatively small pressure difference across the shock and the small value of Γ. Indeed, Landau & Lifshitz (1959) showed that a Taylor-series expansion of the

https://doi.org/10.1017/jfm.2013.13 Published online by Cambridge University Press

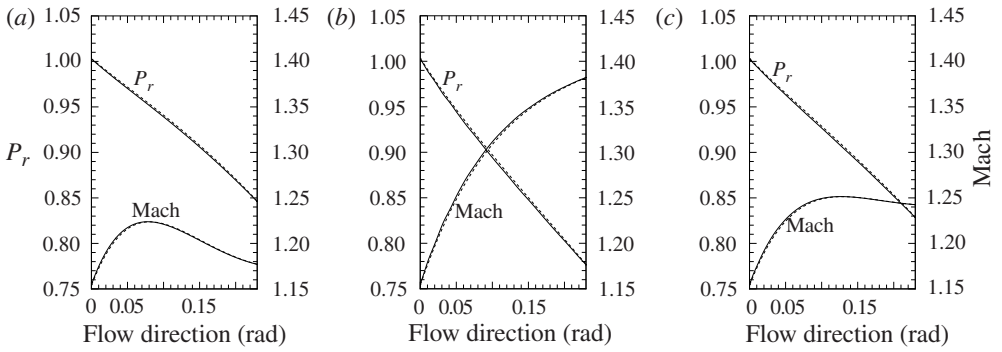


FIGURE 8. Comparison between the numerical integration (– – –) of the Prandtl–Meyer ordinary differential (3.3) and numerical simulation (—): (*a*) MDM; (*b*) MDM (0.75)/MD_6M (0.25); (*c*) MDM (0.40)/MD_6M (0.60).

Rankine–Hugoniot jump conditions delivers the following relation

$$\Delta s \simeq -\frac{\Gamma_A}{6}\frac{c_A^2}{T_A}\left[\frac{\Delta v}{v_A}\right]^3 + o\left(\left[\frac{\Delta v}{v_A}\right]^4\right), \tag{3.4}$$

where $\Delta(\cdot) = (\cdot)_B - (\cdot)_A$, which is valid for weak shock waves. In the present study, the largest entropy difference was computed by solving the nonlinear Rankine–Hugoniot jump conditions for the RSW in MD_6M and it is as small as $\Delta s/s_A \sim 5 \times 10^{-6}$.

To conclude, figure 8 reports the comparison of the numerical integration of the Prandtl–Meyer ordinary differential equation (3.3) and the numerical simulations for the three classical expansions of pure fluid MDM and of the mixtures MDM(0.75)/MD_6M(0.25) and MDM(0.40)/MD_6M(0.60). The very good agreement obtained by these two different approaches increases the authors' confidence on the correctness of the presented results. Furthermore, the values of the upstream and downstream entropy were compared for the three isentropic expansions, for which the exact results is $\Delta s/s_A \equiv 0$ since $s_A \equiv s_B$. Small relative differences of about 10^{-6} confirmed that effects of numerical dissipation were negligible.

4. Conclusions

Non-classical gas dynamic phenomena in dense vapours of organic mixtures have been investigated for the first time. In particular, the effect of non-ideal mixing on the thermodynamic properties relevant to the fluid dynamics was studied.

Predictive EoSs have been used to compute the thermodynamic properties of the mixture, most notably the fundamental derivative of gas dynamics Γ, for mixtures of siloxanes, perfluorocarbons, and siloxanes-perfluorocarbons. Some of the exemplary mixtures display thermodynamic regions of negative nonlinearity for certain compositions. The dependence of the minimum value of Γ in the vapour phase from the molar composition has been analysed in the paradigmatic case of mixtures of linear siloxanes. It is found that Γ_{min} is always greater than the value of Γ_{min} of the most complex molecule in the mixture. In addition, the value Γ_{min} of a pure linear siloxane whose molecular weight is intermediate with respect to that of

https://doi.org/10.1017/jfm.2013.13 Published online by Cambridge University Press

the mixture constituents, is always lower than that of the mixture featuring the same molecular weight or complexity.

Preliminary simulations of a supersonic flow of a dense vapour expanding over a corner are presented. The dense vapour is a binary mixture of linear siloxanes MDM/MD_6M, whereby for each simulation the upstream conditions are kept similar, while the molar composition is varied from $x_{MDM} = 0$ to $x_{MDM} = 1$. The results show how the flow field changes from the classical expansion fan to a RSW, when the composition is MDM(0.05)/MD_6M(0.95). For MDM(0.15)/MD_6M(0.85) a mixed rarefaction shock/fan is predicted. Thermal decomposition of the fluid and critical point effects are to be carefully assessed before selecting the substance for experiments. However, it is remarkable that, similarly to previous studies on non-classical flows, the same gas dynamics behaviour is expected for all considered fluids.

We conclude that for the considered mixtures, mixing compounds of the same fluid family does not enhance non-classical gas dynamic phenomena. Given the variety and complexity of molecular interactions among different molecules, the possibility that the opposite effect occurs for different mixture compositions can not be ruled out. Limitations with respect to accuracy and predictive character of currently available thermodynamic models for mixtures make the analysis of the possibly large variety of mixtures difficult. In addition, these limitations must be considered also with respect to the results of this study.

Future work will be devoted to the improvement of thermodynamic models suitable for complex organic compounds, possibly also by means of property measurements. Indeed, the main obstacle to such investigation is the lack of experimental thermodynamic data of mixtures of complex organic compounds, or of predictive and accurate thermodynamic models, valid close to the vapour–liquid critical point.

Attention will be dedicated to highly non-ideal mixtures in an attempt to understand whether an enhancement of non-classical gas dynamic effects can be achieved by mixing two or more different organic fluids. This possibility, together with thermal stability, would have a large impact on experiments aimed at generating and measuring non-classical gas dynamic phenomena. Siloxane mixtures will also be tested in the experimental facility for generating and measuring RSWs at the Delft University of Technology.

Acknowledgements

This research is supported by the Dutch Technology Foundation STW, and the Technology Program of the Ministry of Economic Affairs, project DSF 11143. The authors acknowledge the contribution of their colleague and friend T.P. van der Stelt for development of the mixture thermodynamic models.

Appendix. iPRSV-WS thermodynamic model

The thermodynamic model adopted for the multi-component fluids is briefly described here. The volumetric EoS is provided by the so-called improved Stryjek–Vera Peng–Robinson (iPRSV) model complemented by a usual polynomial expression for the isobaric ideal-gas specific heat, see van der Stelt (2012), and by the Wong & Sandler (1992) mixing rules.

Stryjek & Vera (1986), see also Proust & Vera (1989), proposed to use the Peng Robinson (Peng & Robinson 1976) cubic EoS, with the Soave (Soave 1972)

https://doi.org/10.1017/jfm.2013.13 Published online by Cambridge University Press

α-function, but with a different temperature and acentric factor dependence in order to improve the correlation of vapor pressures for a wide variety of fluids. Notably, the proposed functional form for α results in the Stryjek–Vera Peng–Robinson (PRSV) EoS featuring a discontinuity in all of the properties at the absolute critical temperature, T_c, for water and alcohols, and at temperature $T = 0.7 \cdot T_c$ for all the other fluids. Recently, van der Stelt (2012) proposed a modification of the PRSV EoS aimed at eliminating the discontinuity in the prediction of thermodynamic properties.

The iPRSV EoS is similar to the cubic form proposed by Peng & Robinson (1976),

$$P = \frac{RT}{v-b} - \frac{a}{v^2 + 2bv - b^2}, \tag{A 1}$$

where

$$a = \left(0.457235\, R^2 T_c^2 / P_c\right) \alpha, \quad b = 0.077796\, R T_c / P_c, \quad \alpha = \left[1 + \kappa \left(1 - \sqrt{T_r}\right)\right]^2. \tag{A 2}$$

Here $R = \mathscr{R}/\mu$ is the gas constant, with $\mathscr{R}$ universal gas constant and μ molecular weight. a is the attractive term, b is the co-volume parameter, P and v are the pressure and the specific volume, respectively. The subscript c indicates properties at the vapour–liquid critical point. The parameter κ depends on the temperature as follows

$$\kappa = \kappa_0 + \kappa_1 \left(1 + \sqrt{T_r}\right) (0.7 - T_r), \tag{A 3}$$

with

$$\kappa_0 = 0.378893 + 1.4897153\omega - 0.17131848\omega^2 + 0.0196554\omega^3, \tag{A 4}$$

where ω is the acentric factor. The empirical parameter κ_1 in (A 3) is a pure-component parameter chosen in order to obtain accurate predictions of saturated properties. From low temperatures up to reduced temperatures of $T_r = 0.7$, Stryjek and Vera recommend using values for κ_1 tabulated in their papers (Stryjek & Vera 1986; Proust & Vera 1989). Alternatively, κ_1 can also be obtained by regressing experimental data. According to Stryjek and Vera, for water and alcohols the tabulated values can be applied up to the critical point. For other compounds, slightly better results are obtained with $\kappa_1 = 0$ for $0.7 < T_r < 1$. For supercritical temperatures ($T_r \geqslant 1$) they recommend $\kappa_1 = 0$, because there would be no advantage in using (A 2) in this region. The κ-function therefore introduces a discontinuity in $\alpha(T)$ either at $T_r = 0.7$ or at $T_r = 1$, and in thermodynamic properties dependent upon and derivatives thereof. The iPRSV EoS is obtained by modifying the equation for the calculation of the κ value, such that it is continuous with the temperature, but by keeping the same parameters κ_0 and κ_1 in the functional form, and in such a way that the same values can be used. This is a notable advantage, because a large amount of data for these parameters that have been obtained so far can still be used. The κ function in the iPRSV thermodynamic model is therefore

$$\kappa = \kappa_0 + \kappa_1 \left\{ \sqrt{\left[A - D\,(T_r + B)\right]^2 + E} + A - D\,(T_r + B) \right\} \sqrt{T_r + C}, \tag{A 5}$$

where the value of the coefficients are $A = 1.1$, $B = 0.25$, $C = 0.2$, $D = 1.2$ and $E = 0.01$. The accuracy of the iPRSV thermodynamic model is similar or better than that of the model (PRSV) from which is derived. The derivatives of κ with respect to the temperature, that are required for the implementation of a complete thermodynamic

https://doi.org/10.1017/jfm.2013.13 Published online by Cambridge University Press

model into a computer program, are given by van der Stelt (2012) together with a thorough discussion on the limits of the thermodynamic model.

Wong & Sandler (1992) developed a set of mixing rules which satisfy the theoretically correct quadratic composition dependence of the second virial coefficient. The mixing rule is derived by equating the excess Helmholtz energy A^{E} of an activity coefficient model describing molecular interaction in the liquid phase to that obtained from the EoS at the so-called infinite-pressure state, namely, in the limit of a specific volume approaching the co-volume. The mixing rule contains one additional binary interaction parameter k_{ij} in the cross second virial coefficient, see (A 9). The binary interaction parameter can be determined by various approaches, see e.g. Coutsikos *et al.* (1995). The Wong–Sandler mixing rule (WSMR) is used extensively in conjunction with the PRSV EoS. For the activity coefficient model, a so-called 'solely energetic' model is usually preferred (i.e. a model which does not have an explicit free-volume term). As it is common practice for the PRSV EoS, the non-random two-liquid (NRTL) model introduced by Renon & Prausnitz (1968) is used here to compute the activity coefficient, see also Ghosh & Taraphdar (1998).

According to the WSMR, the a and b coefficients in (A 1) are substituted by

$$a_M = RTDb_M \quad \text{and} \quad b_M = \frac{Q}{1-D}, \tag{A 6}$$

respectively, where

$$D = \frac{A^{\mathrm{E}}_{\infty}}{C_{EoS}} + \sum_{i=1}^{NC} \frac{x_i a_i}{RTb_i}, \quad Q = \sum_{i=1}^{NC}\sum_{j=1}^{NC} x_i x_j \left(b - \frac{a}{RT}\right)_{ij}. \tag{A 7}$$

The parameter C_{EoS} depends upon the EoS. For the PRSV EoS, it reads

$$C_{EoS} = \frac{\sqrt{2}}{2} \ln\left(\sqrt{2}-1\right) \approx -0.62323. \tag{A 8}$$

The following combining rule has been used

$$\left(b - \frac{a}{RT}\right)_{ij} = \frac{b_i + b_j - a_i + a_j}{2RT}\left(1 - k_{ij}\right) \tag{A 9}$$

where a and b are the energy and the co-volume parameter. The subscript M refers to mixture properties while i and j refer to the components in the mixture and superscript NC denotes the number of components.

From the pressure EoS, a complete thermodynamic model can be finally obtained by specifying the relation between the temperature and the specific heat at constant pressure c_P in the dilute gas limit (see e.g. Callen 1985). In the present study, the following functional form of c_P

$$\psi(T) = \lim_{v\to\infty} c_P(T, v) = C_0 + C_1 T + C_2 T^2 + C_3 T^3 \tag{A 10}$$

with C_0, C_1, C_2 and C_3 constants. The values of the parameters C_0, C_1, C_2 and C_3 are given by van der Stelt (2012) for the fluids of interest here. From the c_P definition (A 10) and the pressure EoS (A 1) a complete thermodynamic model can be obtained.

https://doi.org/10.1017/jfm.2013.13 Published online by Cambridge University Press

For example, from the reciprocity relation, one immediately computes the energy EoS as

$$e(T, v) = \phi(T) + \int_{v_0}^{v} \left[T \frac{\partial P(T, \nu)}{\partial \nu} - P \right] \mathrm{d}\nu \tag{A 11}$$

where, from Meyer's law of ideal gas, $\phi(T) = \psi(R) - R = \lim_{v \to \infty} c_v(T, v)$ is the specific heat at constant volume in the dilute gas limit. All of the thermodynamic variables can be computed from the two pressure and energy EoSs (A 1) and (A 9), respectively, as detailed, e.g. by Colonna & Silva (2003).

REFERENCES

ABBOTT, M. M. 1973 Cubic equations of state. *AIChE J.* **19**, 596–601.

ALDO, A. & ARGROW, B. 1995 Dense gas flow in minimum length nozzles. *Trans. ASME I: J. Fluids Engng* **117** (2), 270–276.

ANGELINO, G. & COLONNA, P. 1998 Multicomponent working fluids for organic Rankine cycles (ORC_S). *Energy* **23** (6), 449–463.

ANGELINO, G. & COLONNA, P. 2000 Air cooled siloxane bottoming cycle for molten carbonate fuel cells. In *Fuel Cell Seminar* pp. 667–670.

ANGELINO, G. & INVERNIZZI, C. 1993 Cyclic methylsiloxanes as working fluids for space power cycles. *Trans. ASME: J. Sol. Energy* **115** (3), 130–137.

ARGROW, B. M. 1996 Computational analysis of dense gas shock tube flow. *Shock Waves* **6**, 241–248.

ARMENIO, A. 2009 Siloxane/perfuorocarbon mixtures as working fuid for organic Rankine cycle turbogenerators. Master's thesis (Report ET-2365), Politecnico di Milano - Delft University of Technology.

BETHE, H. A. 1942 The theory of shock waves for an arbitrary equation of state. Technical Report 545. Office Sci. Res. & Dev.

BORISOV, A. A., BORISOV, AL. A., KUTATELADZE, S. S. & NAKORYAKOV, V. E. 1983 Rarefaction shock waves near the critic liquid–vapour point. *J. Fluid Mech.* **126**, 59–73.

BROWN, B. & ARGROW, B. 1997 Two-dimensional shock tube flow for dense gases. *J. Fluid Mech.* **349**, 95–115.

BROWN, B. & ARGROW, B. 1998 Nonclassical dense gas flows for simple geometries. *AIAA J.* **36** (10), 1842–1847.

BROWN, B. & ARGROW, B. 2000 Application of Bethe–Zel'dovich–Thompson fluids in organic Rankine cycle engines. *J. Propul. Power* **16** (6), 1118–1124.

BYMASTER, A., EMBORSKY, C., DOMINIK, A. & CHAPMAN, W. 2008 Renormalization-group corrections to a perturbed-chain statistical associating fluid theory for pure fluids near to and far from the critical region. *Ind. Engng Chem. Res.* **47** (16), 6264–6274.

CALLEN, H. B. 1985 *Thermodynamics and an Introduction to Thermostatistics*. 2nd edn. Wiley.

CHANDRASEKAR, D. & PRASAD, P. 1991 Transonic flow of a fluid with positive and negative nonlinearity through a nozzle. *Phys. Fluids* A **3** (3), 427–438.

CHEN, H., GOSWAMI, D. Y., RAHMAN, M. M. & STEFANAKOS, E. K. 2011 A supercritical Rankine cycle using zeotropic mixture working fluids for the conversion of low-grade heat into power. *Energy* **36** (1), 549–555.

CINNELLA, P. 2008 Transonic flows of dense gases over finite wings. *Phys. Fluids* **20** (4).

CINNELLA, P. & CONGEDO, P. M. 2007 Inviscid and viscous aerodynamics of dense gases. *J. Fluid Mech.* **580**, 179–217.

CINNELLA, P. & CONGEDO, P. M. 2008 Optimal airfoil shapes for viscous transonic flows of Bethe–Zel'dovich–Thompson fluids. *Comput. Fluids* **37**, 250–264.

COLONNA, P. 1996 Fluidi di lavoro multi componenti per cicli termodinamici di potenza (multicomponent working fluids for power cycles). PhD thesis, Politecnico di Milano.

COLONNA, P. & GUARDONE, A. 2006 Molecular interpretation of nonclassical gas dynamics of dense vapors under the van der Waals model. *Phys. Fluids* **18** (5), 056101.

https://doi.org/10.1017/jfm.2013.13 Published online by Cambridge University Press

COLONNA, P., GUARDONE, A. & NANNAN, N. R. 2007 Siloxanes: a new class of candidate Bethe–Zel'dovich–Thompson fluids. *Phys. Fluids* **19** (8), 086102.

COLONNA, P., GUARDONE, A., NANNAN, N. R. & ZAMFIRESCU, C. 2008*a* Design of the dense gas flexible asymmetric shock tube. *Trans. ASME I: J. Fluids Engng* **130** (3), 034501.

COLONNA, P., NANNAN, N. R. & GUARDONE, A. 2008*b* Multiparameter equations of state for siloxanes: $[(CH_3)_3–Si–O_{1/2}]_2–[O\text{-}Si–(CH_3)_2]_{i=1,\ldots,3}$ and $[O–Si–(CH_3)_2]_6$. *Fluid Phase Equilib.* **263** (2), 115–130.

COLONNA, P., NANNAN, N. R., GUARDONE, A. & LEMMON, E. W. 2006 Multiparameter equations of state for selected siloxanes. *Fluid Phase Equilib.* **244**, 193–211.

COLONNA, P., NANNAN, N. R., GUARDONE, A. & VAN DER STELT, T. P. 2009 On the computation of the fundamental derivative of gas dynamics using equations of state. *Fluid Phase Equilib.* **286** (1), 43–54.

COLONNA, P. & SILVA, P. 2003 Dense gas thermodynamic properties of single and multicomponent fluids for fluid dynamics simulations. *Trans. ASME I: J. Fluids Engng* **125** (3), 414–427.

COLONNA, P., VAN DER STELT, T. P. & GUARDONE, A. 2012 FluidProp (Version 3.0): A program for the estimation of thermophysical properties of fluids. http://www.fluidprop.com/, a program since 2004.

CONGEDO, P., COLONNA, P., CORRE, C., WITTEVEEN, J. & IACCARINO, G. 2012 Backward uncertainty propagation method in flow problems: application to the prediction of rarefaction shock waves. *Comput. Meth. Appl. Engng* **213–216**, 314–326.

COUTSIKOS, P., KALOSPIROS, N. & TASSIOS, D. 1995 Capabilities and limitations of the Wong–Sandler mixing rules. *Fluid Phase Equilib.* **108** (1–2), 59–78.

CRAMER, M. & KLUWICK, A. 1984 On the propagation of waves exhibiting both positive and negative nonlinearity. *J. Fluid Mech.* **142**, 9–37.

CRAMER, M. S. 1989 Negative nonlinearity in selected fluorocarbons. *Phys. Fluids* **1** (11), 1894–1897.

CRAMER, M. S. 1991 Nonclassical dynamics of classical gases. In *Nonlinear Waves in Real Fluids* (ed. A. Kluwick), pp. 91–145. Springer-Verlag.

CRAMER, M. S. & BEST, L. M. 1991 Steady, isentropic flows of dense gases. *Phys. Fluids* **3** (1), 219–226.

CRAMER, M. S. & CRICKENBERGER, A. B. 1991 The dissipative structure of shock waves in dense gases. *J. Fluid Mech.* **223**, 325–355.

CRAMER, M. S. & SEN, R. 1986 Shock formation in fluids having embedded regions of negative nonlinearity. *Phys. Fluids* **29**, 2181–2191.

CRAMER, M. S. & SEN, R. 1987 Exact solutions for sonic shocks in van der Waals gas. *Phys. Fluids* **30** (2), 377–385.

CRAMER, M. S. & SEN, R. 1990 Mixed nonlinearity and double shocks in superfluid helium. *J. Fluid Mech.* **221**, 233–261.

CRAMER, M. S., TARKENTON, L. M. & TARKENTON, G. M. 1992 Critical Mach number estimates for dense gases. *Phys. Fluids* **4** (8), 1840–1847.

DVORNIC, P. R. 2004 In *Silicon Compounds: Silanes and Silicones* High temperature stability of polysiloxanes, pp. 419–432. Gelest Inc.

FERGASON, S. H. 2001 Dense gas shock tube: design and analysis. PhD thesis, University of Colorado, Boulder.

FERGASON, S. H., GUARDONE, A. & ARGROW, B. M. 2003 Construction and validation of a dense gas shock tube. *J. Thermophys. Heat Transfer* **17** (3), 326–333.

FERGASON, S. H., HO, T. L., ARGROW, B. M. & EMANUEL, G. 2001 Theory for producing a single-phase rarefaction shock wave in a shock tube. *J. Fluid Mech.* **445**, 37–54.

GHOSH, P. & TARAPHDAR, T. 1998 Prediction of vapor–liquid equilibria of binary systems using PRSV equation of state and Wong-Sandler mixing rules. *Chem. Eng. J.* **70** (1), 15–24.

GROSS, J. & SADOWSKI, G. 2001 Perturbed-chain SAFT: An equation of state based on a perturbation theory for chain molecules. *Ind. Engng Chem. Res.* **40** (4), 1244–1260.

GUARDONE, A. 2007 Three-dimensional shock tube flows of dense gases. *J. Fluid Mech.* **583**, 423–442.

https://doi.org/10.1017/jfm.2013.13 Published online by Cambridge University Press

GUARDONE, A., ZAMFIRESCU, C. & COLONNA, P. 2010 Maximum intensity of rarefaction shock waves for dense gases. *J. Fluid Mech.* **642** (1), 127–146.

GULEN, S. C., THOMPSON, P. A. & CHO, H. A. 1989 Rarefaction and liquefaction shock waves in regular and retrograde fluids with near-critical end states. In *Adiabatic Waves in Liquid–vapor Systems* pp. 281–290. Springer-Verlag.

HAYES, W. 1960 The basic theory of gasdynamic discontinuities. In *Fundamentals of Gasdynamics: High Speed Aerodynamics and Jet Propulsion* (ed. H. W. Emmons), vol. 3, pp. 416–481. Princeton University Press.

IVANOV, A. G. & NOVIKOV, S. A. 1961 Rarefaction shock waves in iron and steel. *Zh. Eksp. Teor. Fiz.* **40** (6), 1880–1882.

KLUWICK, A. 2001 Theory of shock waves. Rarefaction shocks. In *Handbook of Shockwaves* vol. 1, chap. 3.4, pp. 339–411. Academic Press.

KLUWICK, A. & MEYER, G. 2010 Shock regularization in dense gases by viscous-inviscid interactions. *J. Fluid Mech.* **644**, 473–507.

KUNZ, O., KLIMECK, R., WAGNER, W. & JAESCHKE, M. 2007 2007 The GERG-2004 wide-range equation of state for natural gases and other mixtures *Tech. Rep.* GERG Technical Monograph, vol. 15, VDI-Verlag.

KUTATELADZE, S. S., NAKORYAKOV, V. E. & BORISOV, A. A. 1987 Rarefaction waves in liquid and gas–liquid media. *Annu. Rev. Fluid Mech.* **19**, 577–600.

LAI, N., WENDLAND, M. & FISCHER, J. 2009 Description of linear siloxanes with PC-SAFT equation. *Fluid Phase Equilib.* **283** (1–2), 22–30.

LANDAU, L. D. & LIFSHITZ, E. M. 1959 *Course of Theoretical Physics, Fluid Mechanics*. vol. 6. Pergamon Press.

LANG, W., ALMBAUER, R. & COLONNA, P. 2013 Assessment of waste heat recovery for a heavy-duty truck engine using an ORC turbogenerator. *J. Engng Gas Turbines Power* **135** (4), 042313.

MENIKOFF, R. & PLOHR, B. J. 1989 The Riemann problem for fluid flow of real material. *Rev. Mod. Phys.* **61** (1), 75–130.

MONACO, J., CRAMER, M. & WATSON, L. 1997 Supersonic flows of dense gases in cascade configurations. *J. Fluid Mech.* **330**, 31–59.

NANNAN, N. R., COLONNA, P., TRACY, C. M., ROWLEY, R. L. & HURLY, J. J. 2007 Ideal-gas heat capacities of dimethylsiloxanes from speed-of-sound measurements and ab initio calculations. *Fluid Phase Equilib.* **257** (1), 102–113.

NANNAN, N. R., GUARDONE, A. & COLONNA, P. 2013 On the fundamental derivative of gas dynamics in the vapor–liquid critical region of single-component typical fluids. *Fluid Phase Equilib.* **337**, 259–273.

NANNAN, R. N. & COLONNA, P. 2009 Improvement on multiparameter equations of state for dimethylsiloxanes by adopting more accurate ideal-gas isobaric heat capacities. *Fluid Phase Equilib.* **280** (1–2), 151–152.

PECNIK, R., RINALDI, E. & COLONNA, P. 2012 Computational fluid dynamics of a radial compressor operating with supercritical CO_2. *Trans. ASME: J. Engng Gas Turbines Power* **134**, 122301.

PECNIK, R., TERRAPON, V. E., HAM, F., IACCARINO, G. & PITSCH, H. 2012 Reynolds-Averaged Navier–Stokes Simulations of the Hyshot II Scramjet. *AIAA J.* **50** (8), 1717–1732.

PENG, D. Y. & ROBINSON, D. B. 1976 A new two-constant equation of state. *Ind. Engng Chem. Fundam.* **15** (1), 59–64.

PROUST, P. & VERA, J. H. 1989 PRSV: the Stryjek–Vera modification of the Peng–Robinson equation of state. Parameters for other pure compounds of industrial interest. *Can. J. Chem. Engng.* **67** (1), 170–173.

RENON, H. & PRAUSNITZ, J. M. 1968 Local compositions in thermodynamic excess functions for liquid mixtures. *AIChE J.* **14** (1), 135–144.

SANDLER, S. I. 1989 *Chemical and Engineering Thermodynamics*. 2nd edn. John Wiley and Sons.

SANDLER, S. I. 1993 *Models for Thermodynamic and Phase Equilibria Calculations*. CRC Press.

SCHNERR, G. & MOLOKOV, S. 1994 Exact solutions for transonic flows of dense gases in two-dimensional and axisymmetric nozzles. *Phys. Fluids* **6** (10), 3465–3472.

https://doi.org/10.1017/jfm.2013.13 Published online by Cambridge University Press

SCHNERR, G. & MOLOKOV, S. 1995 Nonclassical effects in two-dimensional transonic flows. *Phys. Fluids* **7** (11), 2867–2875.

SCHNERR, G. H. & LEIDNER, P. 1993*a* Numerical investigation of axial cascades for dense gases. In *PICAST'1–Pacific International Conference on Aerospace Science Technology,* National Cheng Kung University, Taiwan, Republic of China (ed. E. L. Chin), vol. 2, pp. 818–825.

SCHNERR, G. H. & LEIDNER, P. 1993*b* Two-dimensional nozzle flow of dense gases. In *Fluids Engineering Conference* Washington, DC.

SOAVE, G. 1972 Equilibrium constants from a modified Redlich-Kwong equation of state. *Chem. Engng Sci.* **27**, 1197–1203.

STRYJEK, R. & VERA, J. H. 1986 PRSV: An improved Peng–Robinson equation of state for pure compounds and mixtures. *Can. J. Chem. Engng.* **64** (2), 323–333.

THOMPSON, P. A. 1971 A fundamental derivative in gasdynamics. *Phys. Fluids* **14** (9), 1843–1849.

THOMPSON, P. A. 1988 *Compressilbe Fluid Dynamics*. McGraw-Hill.

THOMPSON, P. A. 1991 Liquid–vapor adiabatic phase changes and related phenomena. In *Nonlinear Waves in Real Fluids* (ed. A. Kluwick), pp. 147–213. Springer-Verlag.

THOMPSON, P. A., CAROFANO, G. A. & KIM, Y. G. 1986 Shock waves and phase changes in a large heat capacity fluid emerging from a tube. *J. Fluid Mech.* **166**, 57–96.

THOMPSON, P. A. & LAMBRAKIS, K. C. 1973 Negative shock waves. *J. Fluid Mech.* **60**, 187–208.

THOMPSON, P. A. & LOUTREL, W. F. 1973 Opening time of brittle shock-tube diaphragms for dense fluids. *Rev. Sci. Instrum.* **44** (9), 1436–1437.

TRAPP, C. & COLONNA, P. 2013 Efficiency improvement in pre-combustion CO_2 removal units with a waste-heat recovery ORC power plant. *J. Engng Gas Turbines Power* **135** (4), 04231.

UUSITALO, A., TURUNEN-SAARESTI, T., HONKATUKIA, J., COLONNA, P. & LARJOLA, J. 2013 Siloxanes as working fluids for a mini-ORC systems based on high-speed turbogenerator technology. *Trans. ASME: J. Engng Gas Turbines Power* **135** (4), 042305–042319.

VAN DER STELT, T. P, NANNAN, N. R. & COLONNA, P. 2012 The iPRSV equation of state. *Fluid Phase Equilib.* **330**, 24–35.

VAN DER WAALS, J. D. 1988 *On the Continuity of the Gaseous and Liquid States*. vol. XIV. North-Holland, reprinted.

WEYL, H. 1949 Shock waves in arbitrary fluids. *Commun. Pure Appl. Maths* **2**, 102–122.

WONG, D. S. H. & SANDLER, S. I. 1992 A theoretically correct mixing rule for cubic equations of state. *AIChE J.* **38** (5), 671–680.

ZAMFIRESCU, C., GUARDONE, A. & COLONNA, P. 2008 Admissibility region for rarefaction shock waves in dense gases. *J. Fluid Mech.* **599**, 363–381.

ZEL'DOVICH, Y. 1946 On the possibility of rarefaction shock waves. *Zh. Eksp. Teor. Fiz.* **4**, 363–364.

https://doi.org/10.1017/jfm.2013.13 Published online by Cambridge University Press